BMC Genomics

RESEARCH

Open Access

Ocular A-to-I RNA editing signatures associated with SARS-CoV-2 infection

Yun-Yun Jin[1,2,3,4†], Ya-Ping Liang[1,2,3,4†], Wen-Hao Huang[1,2,3,4], Liang Guo[4], Li-Li Cheng[4], Tian-Tian Ran[4], Jin-Ping Yao[1,2,3,4], Lin Zhu[1,2,3,4] and Jian-Huan Chen[1,2,3,4*]

Abstract

Ophthalmic manifestations have recently been observed in acute and post-acute complications of COVID-19 caused by SARS-CoV-2 infection. Our precious study has shown that host RNA editing is linked to RNA viral infection, yet ocular adenosine to inosine (A-to-I) RNA editing during SARS-CoV-2 infection remains uninvestigated in COVID-19. Herein we used an epitranscriptomic pipeline to analyze 37 samples and investigate A-to-I editing associated with SARS-CoV-2 infection, in five ocular tissue types including the conjunctiva, limbus, cornea, sclera, and retinal organoids. Our results revealed dramatically altered A-to-I RNA editing across the five ocular tissues. Notably, the transcriptome-wide average level of RNA editing was increased in the cornea but generally decreased in the other four ocular tissues. Functional enrichment analysis showed that differential RNA editing (DRE) was mainly in genes related to ubiquitin-dependent protein catabolic process, transcriptional regulation, and RNA splicing. In addition to tissue-specific RNA editing found in each tissue, common RNA editing was observed across different tissues, especially in the innate antiviral immune gene *MAVS* and the E3 ubiquitin-protein ligase *MDM2*. Analysis in retinal organoids further revealed highly dynamic RNA editing alterations over time during SARS-CoV-2 infection. Our study thus suggested the potential role played by RNA editing in ophthalmic manifestations of COVID-19, and highlighted its potential transcriptome impact, especially on innate immunity.

Keywords A-to-I RNA editing, SARS-CoV-2, Ocular surface, Retina, Epitranscriptomic

Introduction

Since 2019, the world has been facing a pandemic of coronavirus disease 2019 (COVID-19) caused by the SARS-CoV-2 virus, resulting in significant impacts on global healthcare and economies [1]. Symptoms of COVID-19 vary from being asymptomatic to severe [2, 3]. SARS-CoV-2 infection could cause viral pneumonia [4], but can also affect the heart, liver, kidney, brain [5–9], and eyes [10]. Understanding such infections in other tissues and organs than the lung is essential for the control and treatment of acute and post-acute COVID-19 sequelae.

The ocular surface is an area directly exposed to the air and thus is vulnerable to possible viral infection. SARS-CoV-2 RNA can be detected in the ocular surface [11], and its viral particles and RNA are detected in different layers of the retina [12, 13]. Additionally, the interaction between spike protein and angiotensin-converting enzyme 2 (*ACE2*) mediates SARS-CoV-2 entry into the human cells, and transmembrane serine protease 2 (*TMPRSS2*) is responsible for the initiation

†Yun-Yun Jin and Ya-Ping Liang contributed equally to this work.

*Correspondence:
Jian-Huan Chen
cjh_bio@hotmail.com
[1] Laboratory of Genomic and Precision Medicine, Wuxi School of Medicine, Jiangnan University, Wuxi, Jiangsu, China
[2] Joint Primate Research Center for Chronic Diseases, Institute of Zoology of Guangdong Academy of Science, Jiangnan University, Wuxi, Jiangsu, China
[3] Jiangnan University Brain Institute, Wuxi, Jiangsu, China
[4] Jiangnan University-Xinshijie Eye Hospital Joint Ophthalmic Research Center, Wuxi, Jiangsu, China

of spike protein and promotes such an interaction [14–17]. ACE2, TMPRSS2, and other accessory entry factors are expressed in the conjunctiva, limbus, cornea, sclera, and retinal organoids [18–20]. Ocular manifestations of COVID-19 include conjunctivitis, keratitis, uveitis, retinitis, etc. [10, 21–35]. However, the underlying mechanisms related to ocular symptoms in COVID-19 remain to be further investigated.

Adenosine-to-inosine (A-to-I) RNA editing mediated by adenosine deaminases that act on RNA (*ADARs*) was the most common canonical RNA editing in mammals [36]. Three members of ADARs are encoded in the human genome, including *ADAR*, *ADARB1*, and *ADARB2*. *ADAR* (also known as *ADAR1*) and *ADARB1* (also known as *ADAR2*) are expressed in many tissues and demonstrate catalytic activity for adenosine deamination, whereas *ADARB2* (also known as *ADAR3*) is mainly present in the brain and no adenosine deaminase activity has been reported [37–39]. As an important component of epigenetics, RNA editing plays an important role in various physiological and pathological processes [40]. It is associated with the pathogenesis of neurodegenerative diseases such as amyotrophic lateral sclerosis (ALS), Parkinson's disease, and Alzheimer's disease [41]. In addition, A-to-I RNA editing is an important component of innate and adaptive immunity and plays an important role in the host's antiviral responses [38], such as those to the Ebola virus, hepatitis virus, SARS, and SARS-CoV-2 [42, 43]. Meanwhile, ADARs influenced SARS-CoV-2 infection in vivo [44]. Moreover, our recent study revealed a possible link between host RNA editing and infection with single-strand RNA viruses, including SARS-CoV-2 in mouse models [45]. However, ocular A-to-I RNA editing during SARS-CoV-2 infection remains uninvestigated in COVID-19 patients.

Herein, we performed a transcriptome-wide analysis to examine the RNA editing profiles of SARS-CoV-2 infections in five ocular tissues, to identify SARS-CoV-2 infection-associated signatures of host RNA editing across tissues. Our findings highlight both the similarities and differences in host RNA editing during SARS-CoV-2 infections and provide valuable insights into the epigenetic mechanisms of RNA editing underlying the ophthalmic manifestations of SARS-CoV-2 infection.

Materials and methods

RNA-Seq dataset downloads

We downloaded three RNA-Seq datasets containing 37 samples of five ocular tissues from the European Nucleotide Archive (ENA) (https://www.ebi.ac.uk/ena). These datasets include PRJNA790648 [46], PRJNA688734 [47], and PRJNA731890 [48]. Dataset PRJNA688734 contains samples from the cornea, limbus, and sclera isolated from human donor tissues and passaged in tissue culture. Cells of the three tissue were infected with SARS-CoV-2 in triplicate and their RNA was collected at 24 h post-infection (hpi), and compared to mock samples ($N=3$ each). The PRJNA790648 contains mock ($N=4$) and SARS-CoV-2 infected ($N=3$) ex vivo cultures of an air–liquid interface organotypic conjunctival epithelial model epithelia infected. Dataset PRJNA731890 [48] contained samlpes of human stem cell-derived retinal organoids that were mock or infected with SARS-CoV-2 collected at 24 and 96 hpi ($N=3$ each). Details of these datasets are shown in Table 1.

Read alignment

The raw sequencing reads were processed using a workflow as previously described [49]. In summary, raw sequencing data quality was assessed using FASTQC [50]. Read alignment was performed using RNA STAR

Table 1 Details of the datasets analyzed in the current study

Bio Project Accession	Tissue	Mock (*N*=18)	Infected (*N*=19)	Viral strain	Multiplicity of infection (MOI)	Incubated time (h)	Contributors	Citation
PRJNA790648	conjunctiva	3	4	BetaCoV/England/2/2020	0.5	24	Jackson, et al., 2022	[46]
PRJNA688734	cornea	3	3	SARS-CoV-2/USA-WA1/2020	1.0	24		
	limbus	3	3				Eriksen, et al., 2021	[47]
	sclera	3	3					
PRJNA731890	retinal organoids (24h)	3	3		0.01	24		
	retinal organoids (96h)	3	3	hCoV19/Germany/FI1103201/2020		96	Menuchin-Lasowski, et al., 2022	[48]

(version 2.7.0e) and the human genome reference sequence (UCSC hg38) [50]. Base quality scores were then recalibrated using GATK (version 4.1.3) [51] after filtering duplicated reads using SAMtools (version 1.9) [52].

RNA editing identification

VarScan (version 2.4.4) and the Ensembl Variant Effect Predictor (VEP) were used for the identification and annotation of A > G single nucleotide variations (SNVs) [53, 54]. SNVs meeting specific criteria were selected, including a base quality of ≥ twenty-five, total sequencing depth of ≥ ten, alternative allele depth of ≥ two, and alternative allele frequency (AAF) of ≥ 1%. SNVs found in the REDIportal V2.0 database were considered high-confidence A-to-I RNA editing sites [55]. Additional filtering criteria were applied to the remaining SNVs, such as excluding those located in homopolymer runs (≥ five nucleotides) or simple repeats, mitochondrial genes, within six nucleotides from splice junctions, within one nucleotide from RNA insertion-deletion (INDEL), within 4% of the ends of reads, annotated as known variants in the dbSNP database Build 142, and those with AAF values of 100% or between 40 and 60% in more than 90% of NC and infected samples. High-confidence A-to-I RNA editing sites were retained for subsequent data analysis, defined as those with editing levels ≥ 1% and observed in two or more samples.

Functional enrichment analysis

Gene Ontology (GO) and Kyoko Encyclopedia of Genes and Genomes (KEGG) pathway analyses were conducted using online prediction tools, including DAVID (https://david.ncifcrf.gov/tools.jsp), Enrichr (https://maayanlab.cloud/Enrichr/), and an online tool (http://www.bioinformatics.com.cn/) [56]. Significance was determined based on a false discovery rate (FDR) < 0.05.

RNA binding protein (RBP) binding site prediction

To gain deeper insights into the potential functional consequences of RNA editing, RBPmap (http://rbpmap.technion.ac.il) was used to predict RNA binding protein sites that coincided with RNA editing sites [57].

Statistical analysis

The general linear model (GLM) and likelihood ratio test were used to compare RNA editing levels between NC and SARS-CoV-2 infected tissues and identify differential RNA editing (DRE), which could be associated with SARS-CoV-2 infection. Empirical *P*-values (P_{GLM}) were calculated using the likelihood ratio test. For sites with P_{GLM} less than 0.05, *Fisher's* exact test was further used to compare the sequencing depth of the reference and alternative alleles in both groups. We applied the Benjamini–Hochberg method to calculate the false discovery rate (FDR). RNA editing sites with FDR less than 0.05 were considered differentially edited. Additionally, we analyzed the correlation between RNA editing and gene expression levels using *Spearman's* correlation.

Results

A-to-I RNA editing profiles in ocular tissues

To assess whether and how ocular A-to-I RNA editing was involved during SARS-CoV-2 infection, we searched and downloaded the publicly available RNA-seq datasets containing ocular tissues or organoids infected with SARS-CoV-2. The results showed the average RNA editing level was decreased in the conjunctiva, limbus, and sclera, but increased in the cornea, with no significant changes between mock and infected retinal organoids (Fig. 1A). Meanwhile, upon infection, *ADAR* expression decreased in the conjunctiva, whereas *ADARB1* expression decreased in the limbus and sclera (Fig. 1B, C). Furthermore, a total of 178558 editing sites were identified in the conjunctiva, 1084 in the limbus, 1140 in the cornea, 941 in the sclera, and 44716 in retinal organoids (Fig. 1D). For the editing genes, 9520, 290, 292, 246, and 3622 were found in conjunctiva, limbus, cornea, sclera, and retinal organoids, respectively (Fig. 1E). Most of these RNA editing sites were in the introns and 3'-untranslated region (UTR) (Fig. 1F). Although missense variants only accounted for a small fraction, they could affect protein structure and stability [58]. So sorts intolerant from tolerant (SIFT) predicted 461 (48.6%), 8 (23.5%), 11 (30.6%), 7 (24.1%), and 134 (32.9%) of the missense variants to be possibly deleterious in the conjunctiva, limbus, cornea, sclera, and retinal organoids, respectively (Fig. 1G). More than half of the repeat sequences of these editing sites were located in the *Alu* repeat elements (Fig. 1H). These results pointed to distinct alterations of RNA editing profiles during SARS-CoV-2 infections.

Comparison of A-to-I RNA editing profiles of SARS-CoV-2 infected ocular tissues

We then looked into the RNA editing profile of each tissue. The five tissue types shared 179 editing sites, and 173,535, 141, 160, 106, and 36,161 specific sites were uniquely found in the conjunctiva, limbus, cornea, sclera, and retinal organoids, respectively (Fig. 2A). For edited genes, 123 were shared by the five tissue types, whereas 6971, 9, 7, 3, and 706 were uniquely observed in the conjunctiva, limbus, cornea, sclera, and retinal organoids, respectively (Fig. 2B). Further comparison of DRE sites and genes among the five tissue types showed 1444, 34, 47, 41, and 1688 tissue-specific DRE sites in the conjunctiva, limbus, cornea, sclera, and retinal organoids,

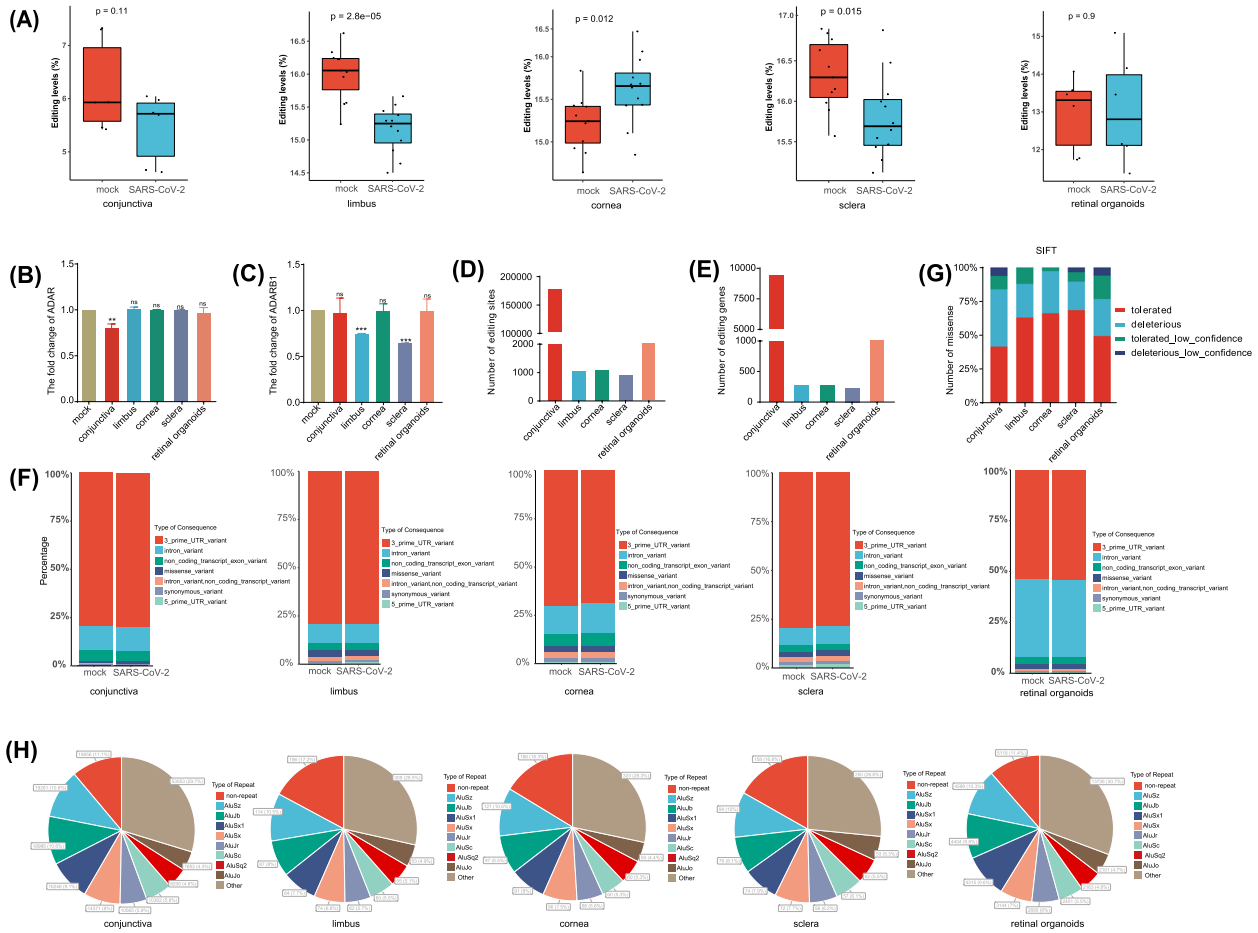

Fig. 1 A-to-I RNA editing was identified from transcriptomes of the five ocular tissues in the current study. **A** The average A-to-I RNA editing level of the conjunctiva, limbus, cornea, sclera, and retinal organoids between mock and SARS-CoV-2 infection. **B**-**C** The fold change in the expression level of *ADAR* and *ADARB1* genes, (**D**-**E**) the number of A-to-I RNA editing sites and genes, and (**F**) the functional types of variants resulting from A-to-I RNA editing in mock and SARS-CoV-2 infection. **G** SIFT prediction of the missense RNA editing variants. **H** RNA editing sites distribution in repetitive elements. A two-tailed unpaired Student's t-test was used to analyze the significance; $^{*}P < 0.05$; $^{**}P < 0.01$; $^{***}P < 0.001$; ns, no significance

respectively (Fig. 2C), and 785, 4, 8, 8, and 580 tissue-specific genes were found in the conjunctiva, limbus, cornea, sclera, and retinal organoids, respectively (Fig. 2D). Notably, the five tissue types shared differential RNA editing in *MAVS* and *MDM2* (Table 2), whereas *LAMP2* (chrX:120,437,993) RNA editing was differentially edited across the conjunctiva, limbus, and sclera (Fig. 2E).

Functional relevance of *SARS-CoV-2 infection-associated* A-to-I RNA editing in ocular tissues

Functional enrichment analysis using these DRE genes was then used to understand the impact of A-to-I RNA editing changes on biological functions during SARS-CoV-2 infection. Notably, the results in Fig. 3 showed more evident functional enrichment of DRE in the conjunctiva and retinal organoids than in the other three tissues included in the current study. The common enrichment in DRE genes consisted of biological processes mainly related to ubiquitin-dependent protein catabolic process, regulation of transcription, RNA splicing, and positive regulation of gene silencing by miRNA (Fig. 3A); common molecular functions mainly related to RNA binding, protein binding, cadherin binding, and metal ion binding (Fig. 3B); common cellular components included the cytosol, nucleoplasm, nucleus, and cytoplasm (Fig. 3C), and common KEGG pathways were mainly related to ubiquitin-mediated proteolysis and herpes simplex virus 1 infection (Fig. 3D). Tissue type also had its unique enriched features, especially those related to viral infection, such as biological processes related to defense response to virus, negative regulation of viral genome replication, and positive regulation of type I interferon-mediated signaling pathway were uniquely found in the cornea, (Fig. 3A), and KEGG pathways of

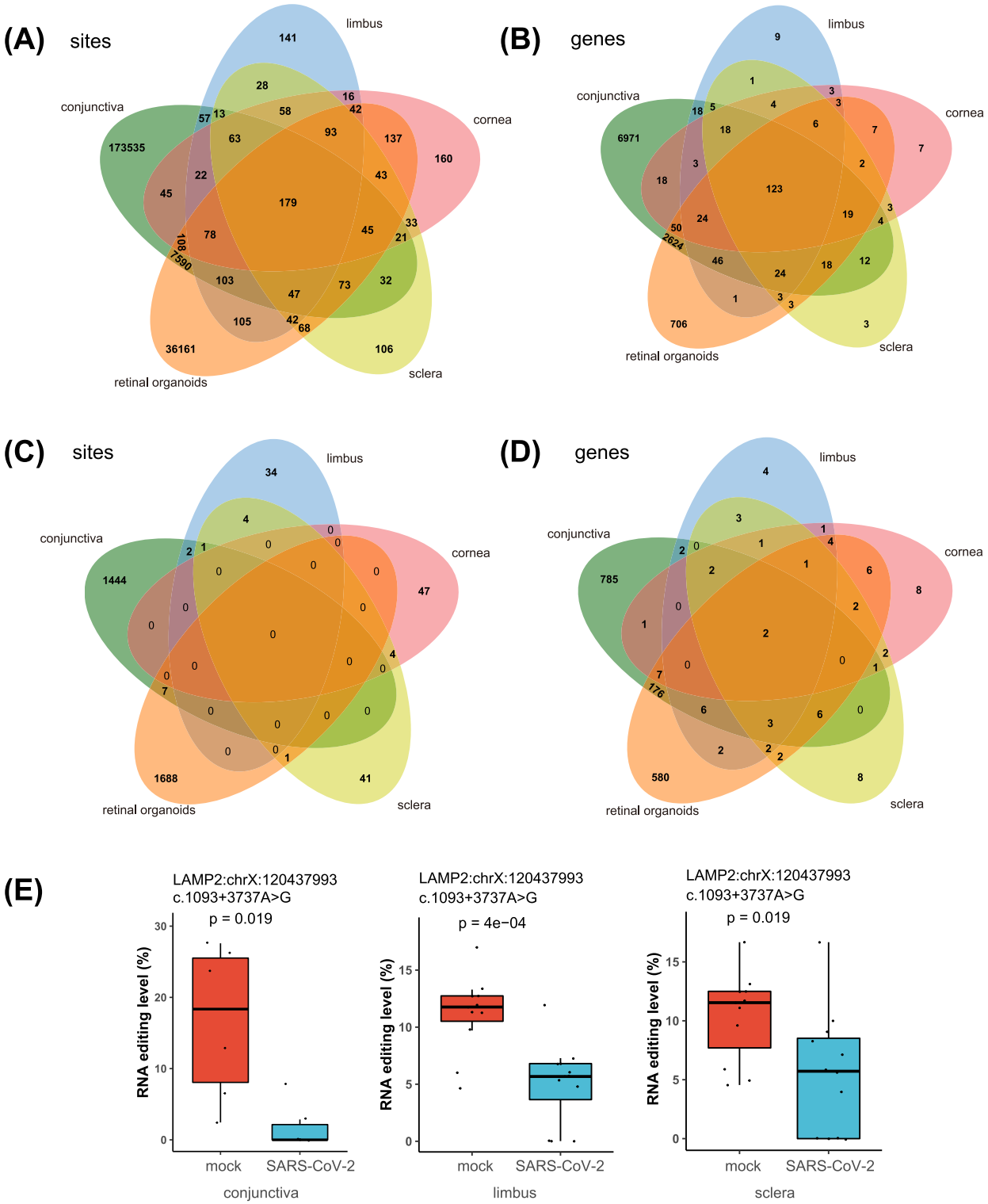

Fig. 2 The similarities and differences of A-to-I RNA editing between the five ocular tissues. **A**-**B** Venn plot showing total A-to-I RNA editing sites (**A**) and genes (**B**) shared by the five ocular tissues. **C**-**D** Venn plot showing differential A-to-I RNA editing sites (**C**) and genes (**D**) shared by five ocular tissues. **E** The editing levels of *LAMP2* (chrX:120,437,993), a common DRE site associated with COVID-19 in the conjunctiva, limbus, and sclera

Table 2 DRE sites in *MDM2* and *MAVS*

Group	Sites	Variants	RNA editing level		*P* value
			mock	infected	
conjunctiva	MDM2:chr12:68843948	3_prime_UTR_variant	5	2.3	0.0059
	MDM2:chr12:68821602	intron_variant	49.1	20.7	0.0070
	MDM2:chr12:68843273	3_prime_UTR_variant	5.3	1.5	0.0199
	MAVS:chr20:3867448	3_prime_UTR_variant	2.9	0.3	6.15E-05
	MAVS:chr20:3871144	3_prime_UTR_variant	21.1	3.9	0.0081
	MAVS:chr20:3873372	3_prime_UTR_variant	5.7	0.8	0.0403
limbus	MDM2:chr12:68843277	3_prime_UTR_variant	11	4.9	0.0362
	MAVS:chr20:3871144	3_prime_UTR_variant	20.2	11.2	0.0251
cornea	MDM2:chr12:68843227	3_prime_UTR_variant	4.4	1.8	0.0496
	MAVS:chr20:3872280	3_prime_UTR_variant	13.1	2.2	0.0010
	MAVS:chr20:3872420	3_prime_UTR_variant	12.5	3.5	0.0216
	MAVS:chr20:3870974	3_prime_UTR_variant	21.4	12	0.0459
sclera	MDM2:chr12:68843230	3_prime_UTR_variant	22.3	34.4	0.0064
	MDM2:chr12:68843729	3_prime_UTR_variant	12.8	5.7	0.0162
	MDM2:chr12:68843244	3_prime_UTR_variant	3.1	8	0.0241
	MAVS:chr20:3867567	3_prime_UTR_variant	15.8	5.7	0.0087
retinal organoids	MDM2:chr12:68843730	3_prime_UTR_variant	9.3	4.1	0.0315
	MAVS:chr20:3867556	3_prime_UTR_variant	5	12.1	0.0019
	MAVS:chr20:3867485	3_prime_UTR_variant	20.6	41.6	0.0104
	MAVS:chr20:3867511	3_prime_UTR_variant	64.5	42.1	0.0318
	MAVS:chr20:3869840	3_prime_UTR_variant	25.7	15.2	0.0460
	MAVS:chr20:3873378	3_prime_UTR_variant	6.1	13.7	0.0475
	MAVS:chr20:3868834	3_prime_UTR_variant	39.8	20.9	0.0476

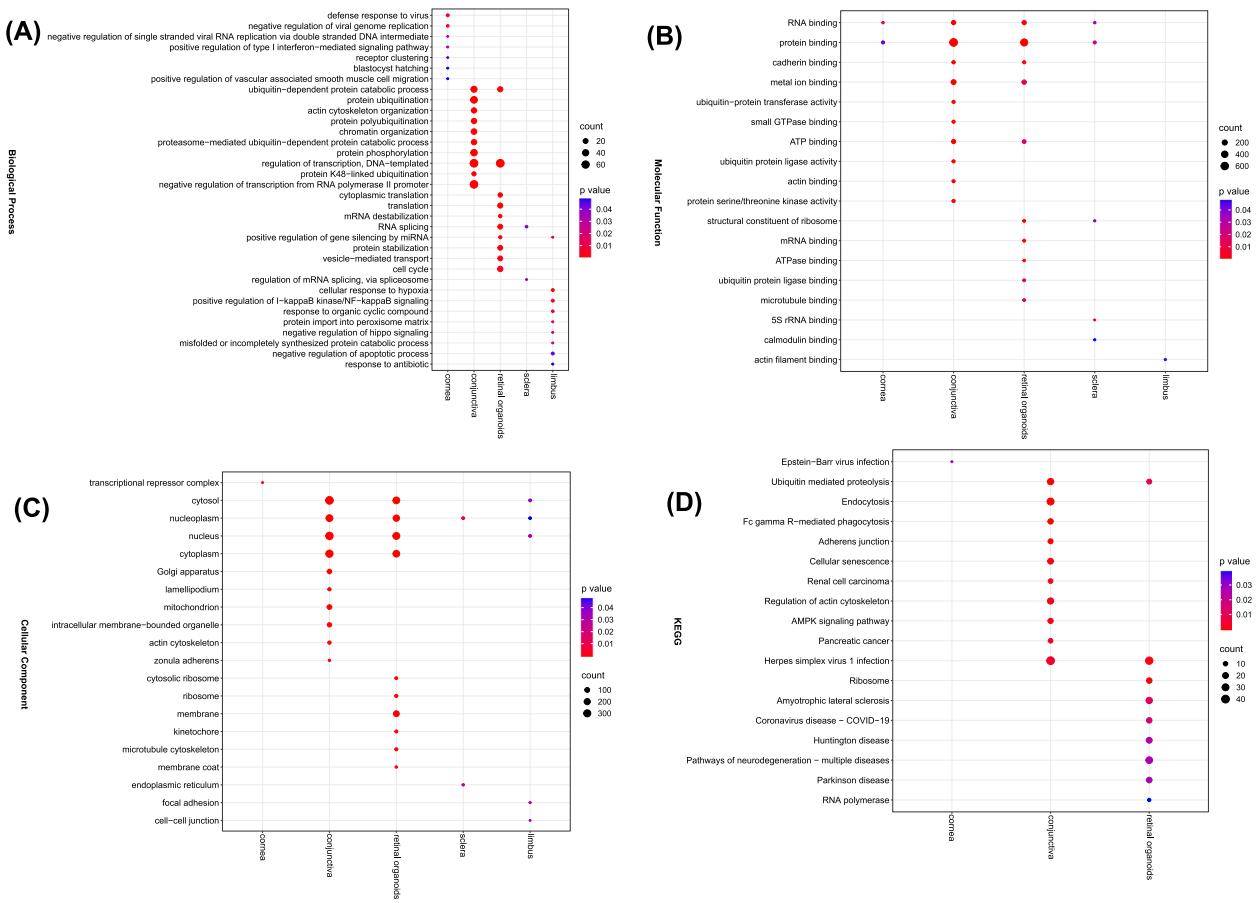

Fig. 3 Functional enrichment analysis of SARS-CoV-2 infection-associated A-to-I RNA editing in the five ocular tissues. **A**-**D** The enrichment analysis results of biological processes (**A**), molecular functions (**B**), cellular components (**C**), and KEGG pathway (**D**) enriched by genes with DRE are shown

coronavirus disease-COVID-19 were unique to the retinal organoids (Fig. 3D).

SARS-CoV-2 infection-associated A-to-I RNA editing in ocular surface tissues

We then focused on the role of A-to-I RNA editing during this process. 1454 DRE sites in 991 genes, 41 DRE sites in 33 genes, 51 DRE sites in 38 genes, and 51 DRE sites in 35 genes were identified in the conjunctiva, limbus, cornea, and sclera infected (Fig. S1). Notably, the top 50 DRE sites (ranked by empirical *P*-values) in the different tissue types (Fig. S2) were strongly correlated with *ADAR* and *ADARB1* expression (Table 3), pointing to an active role of ADARs during ocular infection of SARS-CoV-2. In conjunctiva, the RNA editing levels of DNA polymerase gamma 2 (*POLG2*:chr17:64,495,902), inositol-trisphosphate 3-kinase C (*ITPKC*:chr19:40,729,566), and inflammation and lipid regulator with UBA-like and NBR1-like domains (*ILRUN*:chr6:34,652,970) decreased significantly after SARS-CoV-2 infection (Fig. 4A). In the limbus, the editing level of lysosomal associated membrane protein 2 (*LAMP2*:chrX:120,437,993), SON DNA and RNA binding protein (*SON*:chr21:33,550,969) deceased, and that of collagen type XII alpha 1 chain (*COL12A1*:chr6:75,130,950) increased (Fig. 4B). In the cornea, the editing level of methyltransferase like 7A (*METTL7A*:chr12:5,093,040) deceased after SARS-CoV-2 infection and tripartite motif containing 56 (*TRIM56*:chr7:101,091,531 and chr1:101,091,593) increased after SARS-CoV-2 infection (Fig. 4C). Additionally, both *METTL7A* and *TRIM56* expressions significantly increased after SARS-CoV-2 infection. The editing level and mRNA expression level of *METTL7A* showed a negative correlation, whereas *TRIM56* showed a positive correlation (Fig. S3A-S3D). *SON* (chr21:33,550,969) also showed a decreased editing level in the limbus and sclera upon infection (Fig. 4B, D). Among these sites in the sclera, the most important is that apolipoprotein B mRNA editing enzyme catalytic subunit 3C (*APOBEC3C*), a member of the cytidine deaminase gene family related to C-to-U RNA editing, showed a decreased editing level (Fig. 4D), which was negatively correlated its up-regulated gene expression (Fig. S3E).

Temporal dynamics of A-to-I RNA editing in the retinal organoids during SARS-CoV-2 infection

A total of 1696 DRE sites in 799 DRE genes were identified in the retinal organoids transcriptome upon SARS-CoV-2 infection (Fig. S1). The retinal organoids infected were divided into 24 hpi and 96 hpi groups to investigate the possible role of A-to-I RNA editing during infection. More DRE sites were found at 24 hpi than 96 hpi, with 465 and 272 DRE sites found in 346 and 231 DRE genes at 24 hpi and 96 hpi, respectively (Fig. 5A). These DRE sites varied a lot from 24 to 96 hpi, with only 4 sites and 85 genes shared by 24 hpi and 96 hpi (Fig. 5A). The genes with four common DRE sites included intracisternal A particle-promoted polypeptide (*IPP*:chr1:45,699,736), myocardial infarction associated transcript (*MIAT*:chr22:26,672,672), pleckstrin homology

Table 3 Sites correlated with *ADAR* and *ADARB1*

Group	Editing site	Editing enzyme	Group	Editing site	Editing enzyme
conjunctiva	RUFY3:chr4:70715424	ADAR	conjunctiva	PRKD2:chr19:46708478	ADARB1
	RPS20:chr8:56067442	ADAR		B4GALT5:chr20:49683683	ADARB1
	SYNJ2BP:chr14:70367399	ADAR		**MDM2**:chr12:68821602	ADARB1
	MARCHF2:chr19:8418594	ADAR		CHD9:chr16:53087762	ADARB1
				ITPKC:chr19:40729566	ADARB1
				POLG2:chr17:64495902	ADARB1
				AL024498.2:chr6:10781638	ADARB1
				ILRUN:chr6:34652970	ADARB1
				ANKRD6:chr6:89527467	ADARB1
retinal organoids	SNRPD3:chr22:24573737	ADAR	limbus	LONP2:chr16:48354456	ADARB1
				SON:chr21:33550969	ADARB1
				FGD5-AS1:chr3:14944591	ADARB1
				FLNA:chrX:154351369	ADARB1
				LAMP2:chrX:120437993	ADARB1
				ZYG11B:chr1:52825763	ADARB1
			sclera	**SON:chr21:33550969**	ADARB1
				PAICS:chr4:56459960	ADARB1
				PAICS:chr4:56460959	ADARB1
				APOBEC3C:chr22:39019886	ADARB1
				MDM2:chr12:68843729	ADARB1
			retinal organoids	CROCCP2:chr1:16621015	ADARB1

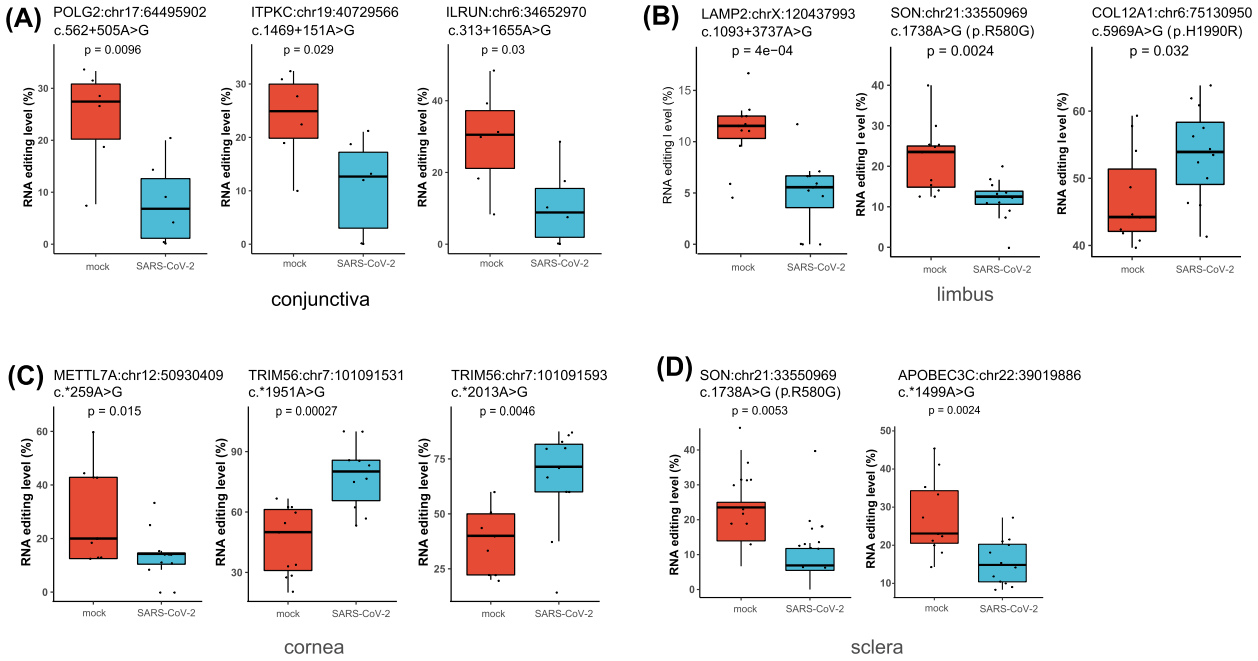

Fig. 4 SARS-CoV-2 infection-associated A-to-I RNA editing in ocular surface tissues. The main DRE sites (no more than 50, ranked by *P*-values) in the conjunctiva (**A**), limbus (**B**), cornea (**C**), and sclera (**D**) are shown

domain containing A5 (*PLEKHA5*:chr12:19,271,334), and caprin family member 2 (*CAPRIN2*:chr12:30,720,208). The editing level of *IPP* and *PLEKHA5* decreased both at 24 hpi and 96 hpi (Fig. 5B). In contrast, the editing levels of *MIAT* and *CAPRIN2* increased both at 24 hpi and 96 hpi compared to mock retinal organoids (Fig. 5B).

Discussion

The COVID-19 pandemic caused by SARS-CoV-2 has affected hundreds of millions worldwide (https://covid19.who.int/). In addition to respiratory symptoms, ocular manifestations are also reported in COVID-19 [10, 21–35]. By conducting a comprehensive epitranscriptomic analysis of ocular tissues, our current study provided evidence supporting the potential role of A-to-I RNA editing in ocular manifestations during SARS-CoV-2 infection.

Our study analyzed RNA sequencing data from publicly available ocular tissue datasets, including the conjunctiva, limbus, cornea, sclera, and retinal organoids, to determine the potential role of A-to-I RNA editing in SARS-CoV-2 infection-related ocular diseases. The results showed significant changes in RNA editing profiles in various ocular tissues after COVID-19 infection. Specifically, the limbus, cornea, and sclera showed fewer RNA editing sites and genes when compared to the conjunctiva and retinal organoids (Fig. 1D, E), possibly due to the lower sequencing depth of the data in the tissues. Although emerging studies have reported ocular symptoms in COVID-19 patients, such as conjunctival congestion, blurred vision, and foreign body sensation [24, 59], it remains unclear how these symptoms are caused by SARS-CoV-2. Our results found that infection with SARS-CoV-2 in ocular tissues substantially altered RNA editing, suggesting a potential role of RNA editing in the ocular infection of SARS-CoV-2 and its ocular manifestations.

Most of these ocular RNA editing sites were within *Alu* repetitive elements (Fig. 1H). *Alu* elements are abundant short interspersed nuclear elements in the human genome and have been shown to play a critical role in regulating gene expression and alternative splicing [60]. In addition, *Alu* elements are also involved in RNA editing as they were hot spots recognized by ADAR enzymes. Our findings suggested that these repetitive elements may play a key role in RNA editing, which contributes to the relationship between RNA editing and ocular SARS-CoV-2 infection.

Common DRE sites were observed in two or more tissues of the conjunctiva, limbus, cornea, sclera, and retinal organoids (Fig. 2C, E). For example, DRE in *LAMP2* was shared among the conjunctiva, limbus, and sclera might suggest the involvement of lysosome-related functions in these tissues during SARS-CoV-2 infection. Importantly, our study also highlighted *MAVS* and *MDM2* genes with common DRE sites across different

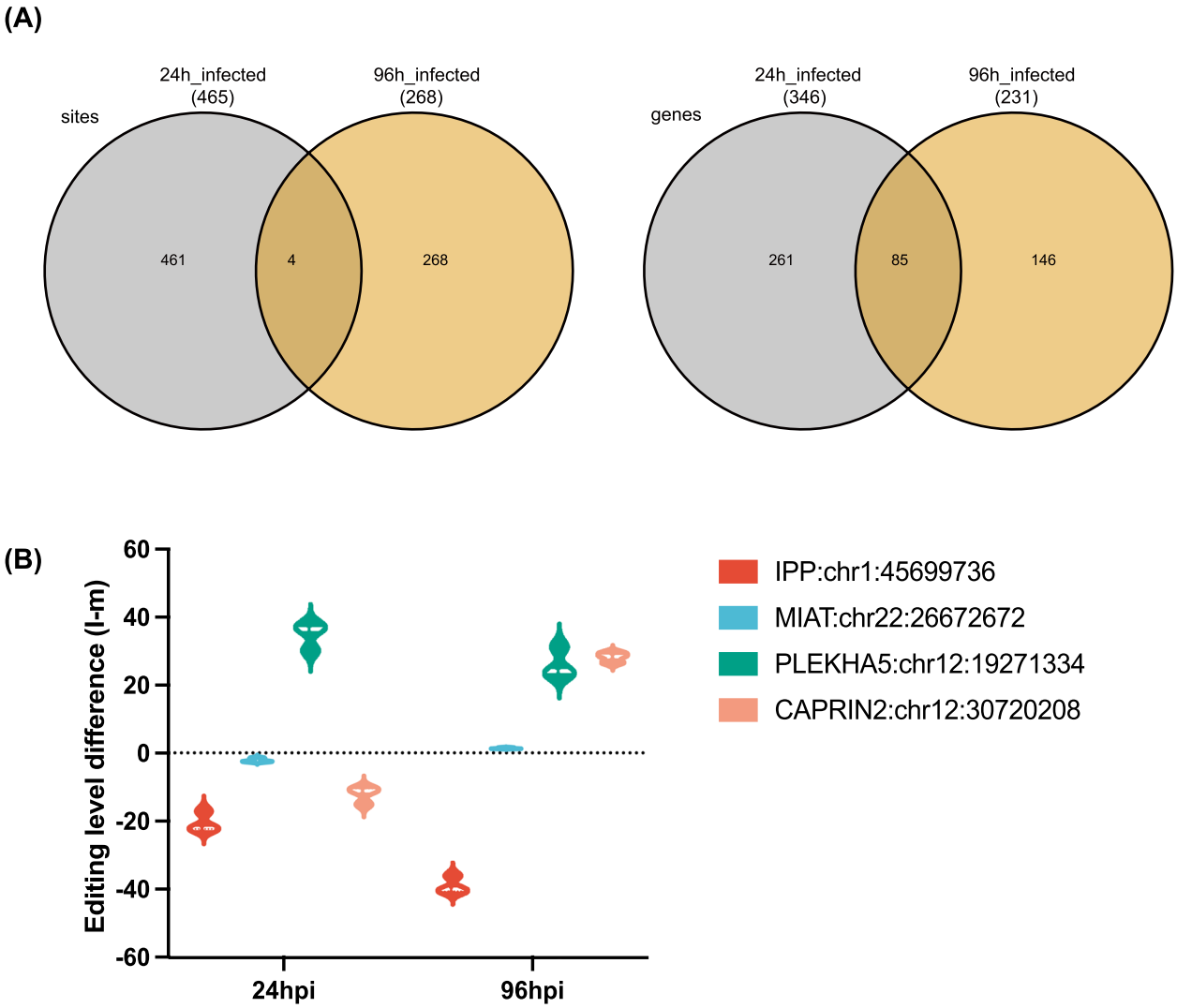

Fig. 5 Temporal dynamics of SARS-CoV-2 infection-associated A-to-I RNA editing in the retinal organoids. **A** 4 sites and 85 genes were shared by 24 hpi and 96 hpi groups, respectively. **B** The editing level difference of four shared sites between 24 and 96 hpi groups

ocular SARS-CoV-2 infections, pointing to common regulatory mechanisms in these tissues during the infection. It has been confirmed that SARS-CoV-2 is involved in the intrinsic antiviral response mediated by MAVS [61], and the inhibition of MDM2 might protect the eye from SARS-CoV-2 infections [62].

Our study also found RNA editing sites significantly correlated with gene expression, suggesting possible *cis*-regulating of gene expression in ocular tissues after SARS-CoV-2 infection. In addition, DRE varied among ocular tissues, particularly the retinal organoids, and conjunctiva, in which SARS-CoV-2 infections might affect the visual and immune functions [63, 64]. In addition, each tissue type had its unique DRE genes, especially those related to viral infections, suggesting a critical yet divergent role of A-to-I RNA editing in the immune response to ocular viral infections due to functional differences among conjunctiva, cornea, and retinal organoids (Fig. 3D).

In addition, we also found that *APOBEC3C* (Fig. 4D), a catalytic subunit of lipoprotein B mRNA editor associated with C-to-U RNA editing, had I-to-I RNA editing level decreased with its gene expression significantly increased. Such a finding might indicate that apart from A-to-I RNA editing, C-to-U RNA editing was also involved in ocular SARS-CoV-2 infections. Studies have shown that *APOBEC3C* is associated with infections of RNA viruses such as hepatitis and HIV [65, 66]. This finding thus implies the involvement of

multiple RNA editing types during SARS-CoV-2 infection, which needs to be explored in further studies.

The study has observed dramatic changes in A-to-I RNA editing in ocular tissues upon SARS-CoV-2 infection. The biological impacts of such epigenetic changes on the eye remain largely undermined and are complex and context-dependent. The effects of such A-to-I RNA editing changes might be beneficial or adverse, depending on specific gene changes, which needs further investigation. Nevertheless, as ADARs and A-to-I RNA editing are considered important antiviral components in mammalian cells, such RNA editing response to SARS-CoV-2 infection is likely to contribute to the cellular antiviral process. For example, the *MAVS* gene showed the most evident changes in RNA editing across different tissues upon the SARS-CoV-2 infection. Interestingly, *MAVS* also showed significant expression changes. *MAVS* encodes a crucial intermediary protein in the virus-induced beta interferon signaling pathways and is essential for activating transcription factors that control the expression of beta interferon and play a role in the innate immune response against viruses [67–69]. Upon SARS-CoV-2 infection, *MAVS* could probably be activated and contribute to the production of interferons, which are key antiviral chemokines that limit viral replication and spread [70, 71]. However, abnormal A-to-I RNA editing has also been recently implicated in diseases, especially immune-related pathogenesis. Persistent SARS-CoV-2 infection might lead to over-activated, A-to-I RNA editing, which could be adverse to the eye. Further research is needed to understand further the consequences of A-I RNA editing in the eye and to determine whether it is ultimately beneficial or adverse.

While providing valuable insights into the potential role of A-to-I RNA editing in ocular manifestations during SARS-CoV-2 infection, our current study has some limitations. Firstly, our study was based on bioinformatics analysis of publicly available datasets, and further experimental validation is needed to confirm the findings. Further functional studies could be important for future perspectives to validate and investigate the functional consequences of the RNA editing changes identified in the current study, which could provide a deeper understanding of the underlying mechanisms. Secondly, the current study focused on A-to-I RNA editing, whereas other types of RNA editing, such as C-to-U editing, which may also play a role in ocular SARS-CoV-2 infections, as well as the interplay between these different types of RNA editing, need to be investigated in further study.

In conclusion, our findings revealed substantial changes in A-to-I RNA editing in ocular tissues upon SARS-CoV-2 infection and provided new insights into understanding ocular manifestations of COVID-19.

Abbreviations

A-to-I	Adenosine to inosine
COVID-19	Coronavirus disease 2019
ACE2	Angiotensin-converting enzyme 2
TMPRSS2	Transmembrane serine protease 2
ADARs	Adenosine deaminases that act on RNA
SNVs	Single nucleotide variations
GO	Gene Ontology
KEGG	Kyoko Encyclopedia of Genes and Genomes
GLM	General linear model
DRE	Differential RNA editing
FDR	False discovery rate
SIFT	Sorts intolerant from tolerant

Supplementary Information

The online version contains supplementary material available at https://doi.org/10.1186/s12864-024-10324-z.

Supplementary Material 1.

Supplementary Material 2.

Supplementary Material 3.

Acknowledgements

We thank Menuchin-Lasowski, Jackson, and Eriksen, et al., for sharing these data.

Authors' contributions

YJ and JC were responsible for the design and writing of the manuscript. YJ and YL conducted the data analysis. The remaining authors engaged in discussions related to the manuscript and made revisions. All authors contributed to the article and approved the final version for submission.

Funding

This study was supported in part by grants from the National Natural Science Foundation of China (No. 82302492, 31671311, 82070987), the National first-class discipline program of Light Industry Technology and Engineering (LITE2018-14), the "Six Talent Peak" Plan of Jiangsu Province (No. SWYY-127), the Innovative and Entrepreneurial Talents of Jiangsu Province, the Program for High-Level Entrepreneurial and Innovative Talents of Jiangsu Province, Natural Science Foundation of Guangdong Province/Guangdong Basic and Applied Basic Research Foundation (2019A1515012062), Taihu Lake Talent Plan, and Fundamental Research Funds for the Central Universities (JUSRP51712B and JUSRP1901XNC), Youth Foundation of Jiangsu Natural Science Foundation (No. BK20190599), Postgraduate Research & Practice Innovation Program of Jiangsu Province (KYCX20_1946), the Fundamental Research Funds for the Central Universities (JUSRP123077), the Wuxi Science and Technology Development Fund Project (K20231035), and Start-Up Research Grants in Medical Colleges (No. 1286010241222110).

Availability of data and materials

The study includes original contributions that are downloaded from the European Nucleotide Archive (ENA) (https://www.ebi.ac.uk/ena), containing 37 samples of five ocular tissues from the PRJNA790648 [46], PRJNA688734 [47], and PRJNA731890 [48]. Any further inquiries or questions can be directed to the corresponding authors of the study.

Declarations

Ethics approval and consent to participate

According to local legislation and institutional requirements, ethical review and approval was not necessary for the study.

Consent for publication
Not applicable.

Competing interests
The authors declare no competing interests.

Received: 12 October 2023 Accepted: 19 April 2024
Published online: 01 May 2024

References

1. Wu Z, McGoogan JM. Characteristics of and Important Lessons From the Coronavirus Disease 2019 (COVID-19) Outbreak in China: Summary of a Report of 72 314 Cases From the Chinese Center for Disease Control and Prevention. JAMA. 2020;323(13):1239–42.
2. Chen N, Zhou M, Dong X, et al. Epidemiological and clinical characteristics of 99 cases of 2019 novel coronavirus pneumonia in Wuhan, China: a descriptive study. Lancet. 2020;395(10223):507–13.
3. Wang D, Hu B, Hu C, et al. Clinical Characteristics of 138 Hospitalized Patients With 2019 Novel Coronavirus-Infected Pneumonia in Wuhan. China Jama. 2020;323(11):1061–9.
4. Cui J, Li F, Shi ZL. Origin and evolution of pathogenic coronaviruses. Nat Rev Microbiol. 2019;17(3):181–92.
5. Adão R, Guzik TJ. Inside the heart of COVID-19. Cardiovasc Res. 2020;116(6):e59–61.
6. Berlin DA, Gulick RM, Martinez FJ. Severe Covid-19. N Engl J Med. 2020;383(25):2451–60.
7. Diao B, Wang C, Wang R, et al. Human kidney is a target for novel severe acute respiratory syndrome coronavirus 2 infection. Nat Commun. 2021;12(1):2506.
8. Jothimani D, Venugopal R, Abedin MF, Kaliamoorthy I, Rela M. COVID-19 and the liver. J Hepatol. 2020;73(5):1231–40.
9. Tay SW, Teh KKJ, Wang LM, Ang TL. Impact of COVID-19: perspectives from gastroenterology. Singapore Med J. 2020;61(9):460–2.
10. Marinho PM, Marcos AAA, Romano AC, Nascimento H, Belfort R Jr. Retinal findings in patients with COVID-19. Lancet. 2020;395(10237):1610.
11. Aiello F, Gallo Afflitto G, Mancino R, et al. Coronavirus disease 2019 (SARS-CoV-2) and colonization of ocular tissues and secretions: a systematic review. Eye (Lond). 2020;34(7):1206–11.
12. Araujo-Silva CA, Marcos AAA, Marinho PM, et al. Presumed SARS-CoV-2 Viral Particles in the Human Retina of Patients With COVID-19. JAMA Ophthalmol. 2021;139(9):1015–21.
13. Casagrande M, Fitzek A, Püschel K, et al. Detection of SARS-CoV-2 in Human Retinal Biopsies of Deceased COVID-19 Patients. Ocul Immunol Inflamm. 2020;28(5):721–5.
14. Hoffmann M, Kleine-Weber H, Schroeder S, et al. SARS-CoV-2 Cell Entry Depends on ACE2 and TMPRSS2 and Is Blocked by a Clinically Proven Protease Inhibitor. Cell. 2020;181(2):271–280.e278.
15. Kuhn JH, Li W, Choe H, Farzan M. Angiotensin-converting enzyme 2: a functional receptor for SARS coronavirus. Cell Mol Life Sci. 2004;61(21):2738–43.
16. Qiu Y, Zhao YB, Wang Q, et al. Predicting the angiotensin converting enzyme 2 (ACE2) utilizing capability as the receptor of SARS-CoV-2. Microbes Infect. 2020;22(4–5):221–5.
17. Yan R, Zhang Y, Li Y, Xia L, Guo Y, Zhou Q. Structural basis for the recognition of SARS-CoV-2 by full-length human ACE2. Science. 2020;367(6485):1444–8.
18. Collin J, Queen R, Zerti D, et al. Co-expression of SARS-CoV-2 entry genes in the superficial adult human conjunctival, limbal and corneal epithelium suggests an additional route of entry via the ocular surface. Ocul Surf. 2021;19:190–200.
19. Ma D, Chen CB, Jhanji V, et al. Expression of SARS-CoV-2 receptor ACE2 and TMPRSS2 in human primary conjunctival and pterygium cell lines and in mouse cornea. Eye (Lond). 2020;34(7):1212–9.
20. Jeong GU, Kwon HJ, Ng WH, et al. Ocular tropism of SARS-CoV-2 in animal models with retinal inflammation via neuronal invasion following intranasal inoculation. Nat Commun. 2022;13(1):7675.
21. Sen M, Honavar SG, Sharma N, Sachdev MS. COVID-19 and Eye: A Review of Ophthalmic Manifestations of COVID-19. Indian J Ophthalmol. 2021;69(3):488–509.
22. Al-Namaeh M. Ocular manifestations of COVID-19. Ther Adv Ophthalmol. 2022;14:25158414221083376.
23. Wu P, Duan F, Luo C, et al. Characteristics of Ocular Findings of Patients With Coronavirus Disease 2019 (COVID-19) in Hubei Province. China JAMA Ophthalmol. 2020;138(5):575–8.
24. Aggarwal K, Agarwal A, Jaiswal N, et al. Ocular surface manifestations of coronavirus disease 2019 (COVID-19): A systematic review and meta-analysis. PLoS ONE. 2020;15(11):e0241661.
25. Costa ÍF, Bonifácio LP, Bellissimo-Rodrigues F, et al. Ocular findings among patients surviving COVID-19. Sci Rep. 2021;11(1):11085.
26. Dong J, Chen R, Zhao H, Zhu Y. COVID-19 and ocular complications: A review of ocular manifestations, diagnostic tools, and prevention strategies. Adv Ophthalmol Pract Res. 2023;3(1):33–8.
27. Douglas KAA, Douglas VP, Moschos MM. Ocular Manifestations of COVID-19 (SARS-CoV-2): A Critical Review of Current Literature. In Vivo. 2020;34(3 Suppl):1619–28.
28. Ho D, Low R, Tong L, Gupta V, Veeraraghavan A, Agrawal R. COVID-19 and the Ocular Surface: A Review of Transmission and Manifestations. Ocul Immunol Inflamm. 2020;28(5):726–34.
29. Hu K, Patel J, Swiston C, Patel BC. Ophthalmic Manifestations of Coronavirus (COVID-19). In: StatPearls. Treasure Island (FL) ineligible companies.
30. Nasiri N, Sharifi H, Bazrafshan A, Noori A, Karamouzian M, Sharifi A. Ocular Manifestations of COVID-19: A Systematic Review and Meta-analysis. J Ophthalmic Vis Res. 2021;16(1):103–12.
31. Yener A. COVID-19 and the Eye: Ocular Manifestations, Treatment and Protection Measures. Ocul Immunol Inflamm. 2021;29(6):1225–33.
32. Zhong Y, Wang K, Zhu Y, et al. Ocular manifestations in COVID-19 patients: A systematic review and meta-analysis. Travel Med Infect Dis. 2021;44:102191.
33. Alnahdi MA, Alkharashi M. Ocular manifestations of COVID-19 in the pediatric age group. Eur J Ophthalmol. 2023;33(1):21–8.
34. Gavriatopoulou M, Korompoki E, Fotiou D, et al. Organ-specific manifestations of COVID-19 infection. Clin Exp Med. 2020;20(4):493–506.
35. Seah I, Agrawal R. Can the Coronavirus Disease 2019 (COVID-19) Affect the Eyes? A Review of Coronaviruses and Ocular Implications in Humans and Animals. Ocul Immunol Inflamm. 2020;28(3):391–5.
36. Witkin KL, Hanlon SE, Strasburger JA, et al. RNA editing, epitranscriptomics, and processing in cancer progression. Cancer Biol Ther. 2015;16(1):21–7.
37. Chen CX, Cho DS, Wang Q, Lai F, Carter KC, Nishikura K. A third member of the RNA-specific adenosine deaminase gene family, ADAR3, contains both single- and double-stranded RNA binding domains. RNA. 2000;6(5):755–67.
38. Lamers MM, van den Hoogen BG, Haagmans BL. ADAR1: "Editor-in-Chief" of Cytoplasmic Innate Immunity. Front Immunol. 2019;10:1763.
39. Song B, Shiromoto Y, Minakuchi M, Nishikura K. The role of RNA editing enzyme ADAR1 in human disease. Wiley Interdiscip Rev RNA. 2022;13(1):e1665.
40. Eisenberg E, Levanon EY. A-to-I RNA editing - immune protector and transcriptome diversifier. Nat Rev Genet. 2018;19(8):473–90.
41. Filippini A, Bonini D, La Via L, Barbon A. The Good and the Bad of Glutamate Receptor RNA Editing. Mol Neurobiol. 2017;54(9):6795–805.
42. Mehedi M, Hoenen T, Robertson S, et al. Ebola virus RNA editing depends on the primary editing site sequence and an upstream secondary structure. PLoS Pathog. 2013;9(10):e1003677.
43. Peng X, Luo Y, Li H, et al. RNA editing increases the nucleotide diversity of SARS-CoV-2 in human host cells. PLoS Genet. 2022;18(3):e1010130.
44. Di Giorgio S, Martignano F, Torcia MG, Mattiuz G, Conticello SG. Evidence for host-dependent RNA editing in the transcriptome of SARS-CoV-2. Sci Adv. 2020;6(25):eabb5813.
45. Wei ZY, Wang ZX, Li JH, et al. Host A-to-I RNA editing signatures in intracellular bacterial and single-strand RNA viral infections. Front Immunol. 2023;14:1121096.
46. Jackson RM, Hatton CF, Spegarova JS, et al. Conjunctival epithelial cells resist productive SARS-CoV-2 infection. Stem Cell Reports. 2022;17(7):1699–713.

47. Eriksen AZ, Møller R, Makovoz B, Uhl SA, tenOever BR, Blenkinsop TA. SARS-CoV-2 infects human adult donor eyes and hESC-derived ocular epithelium. Cell Stem Cell. 2021;28(7):1205–1220.e1207.
48. Menuchin-Lasowski Y, Schreiber A, Lecanda A, et al. SARS-CoV-2 infects and replicates in photoreceptor and retinal ganglion cells of human retinal organoids. Stem Cell Reports. 2022;17(4):789–803.
49. Tao J, Ren CY, Wei ZY, Zhang F, Xu J, Chen JH. Transcriptome-Wide Identification of G-to-A RNA Editing in Chronic Social Defeat Stress Mouse Models. Front Genet. 2021;12:680548.
50. Dobin A, Gingeras TR. Mapping RNA-seq Reads with STAR. Curr Protoc Bioinformatics. 2015;51:11.14.11–11.14.19.
51. Van der Auwera GA, Carneiro MO, Hartl C, et al. From FastQ data to high confidence variant calls: the Genome Analysis Toolkit best practices pipeline. Curr Protoc Bioinformatics. 2013;43(1110):11.10.11–11.10.33.
52. Li JB, Levanon EY, Yoon JK, et al. Genome-wide identification of human RNA editing sites by parallel DNA capturing and sequencing. Science. 2009;324(5931):1210–3.
53. Koboldt DC, Zhang Q, Larson DE, et al. VarScan 2: somatic mutation and copy number alteration discovery in cancer by exome sequencing. Genome Res. 2012;22(3):568–76.
54. McLaren W, Gil L, Hunt SE, et al. The Ensembl Variant Effect Predictor. Genome Biol. 2016;17(1):122.
55. Mansi L, Tangaro MA, Lo Giudice C, et al. REDIportal: millions of novel A-to-I RNA editing events from thousands of RNAseq experiments. Nucleic Acids Res. 2021;49(D1):D1012–d1019.
56. Kuleshov MV, Jones MR, Rouillard AD, et al. Enrichr: a comprehensive gene set enrichment analysis web server 2016 update. Nucleic Acids Res. 2016;44(W1):W90–97.
57. Paz I, Kosti I, Ares M Jr, Cline M, Mandel-Gutfreund Y. RBPmap: a web server for mapping binding sites of RNA-binding proteins. Nucleic Acids Res. 2014;42(Web Server issue):W361–367.
58. Nishikura K. Functions and regulation of RNA editing by ADAR deaminases. Annu Rev Biochem. 2010;79:321–49.
59. Chen X, Yu H, Mei T, et al. SARS-CoV-2 on the ocular surface: is it truly a novel transmission route? Br J Ophthalmol. 2021;105(9):1190–5.
60. Batzer MA, Deininger PL. Alu repeats and human genomic diversity. Nat Rev Genet. 2002;3(5):370–9.
61. Fu YZ, Wang SY, Zheng ZQ, et al. SARS-CoV-2 membrane glycoprotein M antagonizes the MAVS-mediated innate antiviral response. Cell Mol Immunol. 2021;18(3):613–20.
62. Zauli G, AlHilali S, Al-Swailem S, Secchiero P, Voltan R. Therapeutic potential of the MDM2 inhibitor Nutlin-3 in counteracting SARS-CoV-2 infection of the eye through p53 activation. Front Med (Lausanne). 2022;9:902713.
63. Masland RH. The neuronal organization of the retina. Neuron. 2012;76(2):266–80.
64. Shen S, Lin L, Cai JJ, et al. Widespread establishment and regulatory impact of Alu exons in human genes. Proc Natl Acad Sci U S A. 2011;108(7):2837–42.
65. Jaguva Vasudevan AA, Balakrishnan K, Gertzen CGW, et al. Loop 1 of APOBEC3C Regulates its Antiviral Activity against HIV-1. J Mol Biol. 2020;432(23):6200–27.
66. Khalfi P, Suspène R, Caval V, et al. APOBEC3C S188I Polymorphism Enhances Context-Specific Editing of Hepatitis B Virus Genome. J Infect Dis. 2022;226(5):891–5.
67. Kawai T, Takahashi K, Sato S, et al. IPS-1, an adaptor triggering RIG-I- and Mda5-mediated type I interferon induction. Nat Immunol. 2005;6(10):981–8.
68. Liu B, Zhang M, Chu H, et al. The ubiquitin E3 ligase TRIM31 promotes aggregation and activation of the signaling adaptor MAVS through Lys63-linked polyubiquitination. Nat Immunol. 2017;18(2):214–24.
69. Seth RB, Sun L, Ea CK, Chen ZJ. Identification and characterization of MAVS, a mitochondrial antiviral signaling protein that activates NF-kappaB and IRF 3. Cell. 2005;122(5):669–82.
70. Wang M, Zhao Y, Liu J, Li T. SARS-CoV-2 modulation of RIG-I-MAVS signaling: Potential mechanisms of impairment on host antiviral immunity and therapeutic approaches. MedComm Futur Med. 2022;1(2):e29.
71. Zotta A, Hooftman A, O'Neill LAJ. SARS-CoV-2 targets MAVS for immune evasion. Nat Cell Biol. 2021;23(7):682–3.

Publisher's Note